Current Research in Food Science 6 (2023) 100415

Contents lists available at ScienceDirect

Current Research in Food Science

journal homepage: www.sciencedirect.com/journal/current-research-in-food-science

Quality changes and indicator proteins of *Litopenaeus vannamei* based on label-free proteomics analysis during partial freezing storage

Kangting Sun [a,b,c,e], Chuang Pan [a,b,e,*], Shengjun Chen [a,b,d,e,**], Shucheng Liu [c], Shuxian Hao [a,b,e], Hui Huang [a,b,e], Di Wang [a], Huan Xiang [a]

[a] Key Laboratory of Aquatic Product Processing, Ministry of Agriculture and Rural Affairs, National Research and Development Center for Aquatic Product Processing, South China Sea Fisheries Research Institute, Chinese Academy of Fishery Sciences, Guangzhou, 510300, China
[b] Co-Innovation Center of Jiangsu Marine Bio-industry Technology, Jiangsu Ocean University, Lianyungang, 222005, China
[c] College of Food Science and Technology, Guangdong Ocean University, Zhanjiang, 524088, China
[d] Key Laboratory of Efficient Utilization and Processing of Marine Fishery Resources of Hainan Province, Sanya Tropical Fisheries Research Institute, Sanya, 572018, China
[e] Collaborative Innovation Center of Seafood Deep Processing, Dalian Polytechnic University, Dalian, 116034, China

ARTICLE INFO

Keywords:
Label-free proteomics
Litopenaeus vannamei
Partial freezing
Muscle quality
Deterioration

ABSTRACT

Litopenaeus vannamei are known to deteriorate in quality during low-temperature storage. This study demonstrated the potential protein indicators of partial freezing of stored shrimp by traditional quality parameters and label-free based proteomic techniques. The carbonyl content and myofibril fragmentation index (MFI) of shrimp increased from 0.56 ± 0.03 to 2.14 ± 0.03 nmol/mg and 13.09 ± 0.14 to 54.93 ± 0.96, respectively. Within the extension of storage, the trichloroacetic acid (TCA), cooking loss and whiteness significantly increased. A total of 240 proteins changed in abundance at 10, 20, and 30 days compared to fresh samples. Projectin, ribosomal protein and histone were potential biomarkers for protein denaturation and oxidation in shrimp muscle. Myosin heavy chain and glyceraldehyde-3-phosphate dehydrogenase corresponded with the degradation of muscle proteins. Myosin light chain, tubulin alpha chain, and heat shock protein correlated with tenderness and water holding capacity; meantime, malate dehydrogenase and hemocyanin can serve as color indicators. Further study of the properties of these indicator proteins can inform their exploitation as quality indicator proteins during partial freezing storage.

1. Introduction

The Pacific white shrimp (*Litopenaeus vannamei*) is a profoundly popular aquaculture species with consumers because of its giant nutritional and protein content. The highest crude protein content in shrimp muscle was found at 15.09% in *Litopenaeus vannamei*. The high content of crude protein in shrimp muscle is one of the reasons why shrimp is high-quality seafood (Liu et al., 2021a). *L. vannamei* has the advantages of strong reproduction, fast growth, and strong disease resistance, making up an annual harvest of 1.98 million tons in 2022 China (Anonymous, 2022). Simultaneously, *L. vannamei* is becoming one of the most important internationally traded fishery products and an economically aquatic resource because of its growing farm production and economic significance (Chen et al., 2020).

It is well known that temperature control in the food supply chain is an essential aspect of food quality assurance. Low temperatures can inhibit enzyme activity, lipid oxidation, and microbial growth to ensure the quality of aquatic products. Partial freezing is the process of freezing food by lowering the temperature of the product to 1 or 2 °C below its initial freezing point (Lu et al., 2015). Compared to frozen storage, partial freezing allows less of the internal water to freeze, reducing damage to the muscle structure. Higher quality can be obtained when partial freezing products rather than frozen (Gallart-Jornet et al., 2007). However, quality deterioration of shrimp muscle occurs in partial freezing storage (Pan et al., 2019). Low temperature induces the growth of ice crystals in muscle tissue, leading to the release of free water (drip

* Corresponding author. Co-Innovation Center of Jiangsu Marine Bio-industry Technology, Jiangsu Ocean University, Lianyungang, 222005, China.
** Corresponding author. Key Laboratory of Aquatic Product Processing, Ministry of Agriculture and Rural Affairs, National Research and Development Center for Aquatic Product Processing, South China Sea Fisheries Research Institute, Chinese Academy of Fishery Sciences, Guangzhou, 510300, China.
E-mail addresses: silverpfoxc@hotmail.com (C. Pan), chenshengjun@scsfri.ac.cn (S. Chen).

https://doi.org/10.1016/j.crfs.2022.100415
Received 19 September 2022; Received in revised form 26 November 2022; Accepted 9 December 2022
Available online 10 December 2022

loss) and degradation of the textural properties of the shrimp muscle (Zhang et al., 2020a). With the ice crystal growth, the shrimp muscle underwent protein degradation, decreased water holding capacity, and weakened fibrous and connective tissue (Xiang et al., 2022). The effect of crystal growth on protein degradation should be studied systematically.

Quantitative proteomics is an analytical chemistry technique that applies a mass spectrometry platform to detect the relative protein content of sample species. The development of the proteomic analysis technique makes studying detailed protein degradation easier. The isobaric tags for relative and absolute quantification (iTRAQ) technology can simultaneously identify and quantify proteins in 4–8 different samples thereby increasing throughput and reducing experimental error (Shi et al., 2018). However, more than 8 samples will be batched on the machine to produce different batch effects. Label-free protein quantification is a technique that does not rely on isotopic labeling quantified by enzymatic digestion of peptides and integration of the intensity of the ion peaks detected in the resulting mass spectrometry data in terms of integrated area (Xiang et al., 2022). Zhang et al. (2020b) found substantial protein changes which may be associated with cold temperature resistance in *L. vannamei* after 30 days under frozen storage by label-free proteomics analysis. Muscle protein degradation during frozen storage was delayed in the sodium trimetaphosphate pre-soaked group (Zhang et al., 2020b). Lin et al. (2021) used the label-free proteomic analysis to analyze the mechanism of hydroxyl radical-induced protein oxidation in the muscle of *L. vannamei*. The differential proteins identified by the ribosomal protein subunits, putative cytoskeleton proteins and ion-binding proteins are mainly caused by the degradation of structural proteins and changes in protein structure and conformation caused by hydroxyl radical attack in oxidative stress.

Different proteomic techniques have been used to study changes in shrimp muscle, and the identified differential proteins are related to quality changes. However, there are few studies on the changes in shrimp muscle quality under partial freezing. Therefore, this study aimed to investigate the protein changes in shrimp muscle and demonstrate the potential indicator proteins associated with shrimp quality under partial freezing storage by label-free proteomics strategy.

2. Materials and methods

2.1. Chemicals

Lysate L3 and Lysate L3 (with SDS) were purchased from Huijun Biologicals, Guangzhou, China. Shanghai Biotech, Shanghai, China, acquired phenylmethylsulfonyl fluoride (PMSF). Tris (2-carboxyethyl) phosphine (TCEP), Methyl methanethiosulfonate (MMTS), formic acid, and ammonium bicarbonate were provided by Sigma, Shanghai, China. Trypsin was purchased from Promega, WI, USA. Other reagents are analytically pure.

2.2. Sample preparation

Live shrimps with 13 ± 0.5 cm in length and 13 ± 1 g in weight were purchased from the local market and transported to the laboratory in oxygen bags. Shrimps were sacrificed with crushed ice and then washed with running water, removing the heads and surface water of the shrimp. Shrimps were randomly divided into four groups and sealed in Ziplock bag and stored in a refrigerator a −3 °C, and samples were removed for experiments on 0, 10, 20, and 30 days.

2.3. Quality indicators

2.3.1. Determination of color and cooking loss

A colorimeter mini was used to determine the lightness (L*), redness (a*), and yellowness (b*) of shrimp and calculate whiteness according to the formula of Shi et al. (2020). As Wang et al. (2019) described, the cooking loss was determined with slight modification. The cooking time changed to 100 °C for 3 min. The samples were dried with filter paper and weighed after reaching room temperature. The weight difference between raw and cooked samples was defined as cooking loss.

2.3.2. Determination of carbonyl content, TCA soluble peptides and MFI

Carbonyl content was measured by the protein carbonyl assay kit (Jiancheng Bioengineering Institute, Nanjing, China). TCA soluble peptides were determined by the method of Jiang et al. (2021).

The MFI was measured according to the method of Jiang et al. (2021) with slight modifications. One gram of minced muscle was homogenized by adding 15 mL pre-cooled MFI buffer (100 mM KCl, 11.2 mM K_2HPO_4, 8.8 mM KH_2PO_4, 1 mM EGTA, 1 mM $MgCl_2$), passing a 200mesh filter, centrifuged at 1000×*g* for 15 min at 2 °C and the supernatant was discarded. Add again 15 mL MFI buffer, and repeat the above operation. Finally, the precipitate was adjusted to 0.5 mg/mL with MFI buffer, measuring the absorbance at 562 nm with an enzyme labeling measuring instrument (Sunrise-basic Tacan, TECAN, Swiss). The average absorbance times 200 was regarded as the MFI value.

2.4. Label free quantitative proteomics

2.4.1. Protein extraction

Shrimp muscle and lysate L3 with SDS (added 1 × PMSF before use) added in the ratio of 1:10, dissolved and transferred to a 1.5 mL Eppendorf (EP) tube ultrasound (power 600 w, interval 1 s, time 1.5 s, ultrasound 5 min), centrifuged at 12000×*g* for 20 min at 4 °C. Add 250 μL of supernatant to a tube containing 1 ml of acetone and precipitate overnight at −20 °C. The precipitated protein was centrifuged at 12000×*g* for 20 min at 4 °C, and the supernatant was poured off and dried to obtain the processed protein masses. According to the instructions, the concentration of extracted proteins was determined using the Bradford assay kit (Beyotime Biotechnology, Shanghai, China).

2.4.2. Protein digestion

The protein solution was added with 4 μL 50 mM TCEP, reduced at 60 °C for 1 h, and soon afterwards added to 2 μL 55 mM MMTS and protected from light at room temperature for 45 min. Next, the protein was added to a 10 kDa ultrafiltration tube, centrifuged at 12000×*g* for 20 min. Added 100 μL 8 M urea (pH 8.5) to tube, centrifuged at 12000×*g* for 20 min and twice centrifuged. Then added 100 μL 250 mM tetraethylammonium bromide (TEAB) was added, centrifuged at 12000×*g* for 20 min and repeated three times. Later, 50 μL 500 mM TEAB and 2% trypsin was added, and incubated at 37 °C overnight (12 h); next day supplemented with 1% trypsin, incubated at 37 °C for 4 h. Finally replaced with a new collection tube, the filtrate was collected by centrifugation and dried by vacuum at low temperature for HPLC-MS/MS analysis.

2.4.3. Mass spectrometry

The peptides were dissolved in sample lysis solution (0.1% formic acid, 2% acetonitrile) and then centrifuged at 13,000×*g* for 20 min at 4 °C. The supernatant was extracted for mass spectrometric identification. Liquid phase parameters in the column information: RSLC C18 (5 μm), C18 (3 μm, 75 μm × 150 mm); mobile phase information: mobile phase A is 0.1% formic acid, mobile phase B is 0.1% formic acid, 80% acetonitrile, the flow rate is 300 nL/min. The analysis time was 120 min, and the experimental gradient B phase was increased from 5% to 90%. The separated peptides were directly fed into the mass spectrometer Thermo Scientific Q Exactive for online detection.

2.5. Bioinformatics analysis

The database is downloaded from Uniprot, and the MaxQuant Software integrates the LFQ algorithm by extracting the isotopic peaks of each peptide in each analysis. The MaxQuant platform calculates the

protein ratios using the median of the peptide ratios common to all analyses, representing a relatively approximate estimate of the protein ratios. The "peptides.txt" and "proteinGroups.txt" files obtained from MaxQuant analyses are filtered out for site-only, reverse database and common contaminant database.

2.6. Statistical analysis

All measurements were taken in triplicate and expressed as the mean ± SD of three parallel measurements. Data processing and plotting were performed using software such as SPSS 25.0 and Origin. The within-group significance analysis was performed using Ducan multiple analysis, with $p < 0.05$ indicating significant differences.

3. Results and discussion

3.1. Changes in the quality indicators

The generation of the carbonyl groups in protein molecules is considered to be one of the universal features of such oxidative denaturation (Varma and Devamanoharan 1995). MFI is a quick and simple tool to assess muscle tenderness (Rajagopal and Oommen, 2014). As shown in Table 1, Carbonyl content and MFI were significantly increased ($p < 0.05$) with increasing storage time. Carbonyl content increased from 0.56 ± 0.03 nmol/mg in 0 day–2.14 ± 0.03 nmol/mg in 30 days. The initial value of MFI was 13.09 ± 0.14, and rose to 54.93 ± 0.96 after 30 days. The formation of carbonyl groups is usually associated with conformational changes in myogenic fibronectin, which leads to protein fragmentation and aggregation, as well as loss of physicochemical and functional properties (Nikoo et al., 2016). The increasing of MFI revealing that the protein network is disrupted. The strength of protein network is reduced, especially the coarse filaments in the membranes constituting muscle fiber bundles were easier to dissolve, leading to an increase in MFI values (Du et al., 2021).

TCA soluble peptide is commonly used to indicate the extent of protein degradation in postmortem muscle (Benjakul et al., 2003). As illuminated in Table 1, TCA soluble peptide was increased significantly ($p < 0.05$) from 0 to 20 days, but there was no difference ($p > 0.05$) between the 20 days and 30 days groups. TCA soluble peptide content increase indicates autolytic degradation of protein in shrimp muscle during storage (Benjakul et al., 2003; Cho et al., 2012). The production of TCA soluble peptides in shrimps was effectively inhibited at lower temperatures and did not change significantly in the later stages of storage (Lu et al., 2015). As illuminated in Table 1, cooking loss were significantly increased ($p < 0.05$) with increasing storage time. The formation of some ice crystals during partial freezing leads to increased water loss (Wang et al., 2019). Water holding capacity (WHC) refers to the muscle's ability to hold both inherent and added water, which affects the further processing and edible quality of products and consumer acceptance. WHC is closely related to taste, tenderness, color, and other muscle quality features (Liu et al., 2021b; Yang et al., 2022).

Whiteness is one of the most critical parameters affecting the sensory evaluation of customers. During partial freezing, whiteness showed no significant change under 10 days of storage, but there was a significant increase from 31.51 ± 1.58 to 36.36 ± 0.53 from 10 days to 30 days ($p < 0.05$). The increase in whiteness was closely associated with the breakdown of myoglobin in white muscle products; meanwhile, the increase in free water on the product surface also had a whitening effect (Shi et al., 2020).

Table 1
Quality indicators in 0 days, 10 days, 20 days, and 30 days of *L. vannamei* during partial freezing when 0 day was controlled sample and 10 days, 20 days, 30 days were experimental group.

Item	0 day	10 days	20 days	30 days
Carbonyl content (nmol/mg)	0.56 ± 0.03 ^{a}	1.26 ± 0.04 ^{b}	1.38 ± 0.08 ^{c}	2.14 ± 0.03 ^{d}
MFI	13.09 ± 0.14 ^{a}	20.13 ± 0.09 ^{b}	46.47 ± 1.05 ^{c}	54.93 ± 0.96 ^{d}
TCA-soluble peptides (μmol tyr g^{-1} muscle)	1.48 ± 0.08 ^{c}	3.82 ± 0.09 ^{b}	5.83 ± 0.07 ^{a}	6.02 ± 0.09 ^{a}
Cooking loss (%)	12.99 ± 0.52 ^{a}	21.37 ± 0.55 ^{b}	21.93 ± 0.61 ^{bc}	22.55 ± 0.40 ^{c}
Whiteness	31.61 ± 1.18 ^{a}	31.51 ± 1.58 ^{a}	34.13 ± 0.74 ^{b}	36.36 ± 0.53 ^{c}

3.2. Identification of proteins

Shrimps muscle stored for 0 days, 10 days, 20 days, and 30 days were selected for proteomic analysis. Total of 612 proteins and 4702 peptides were identified through label-free proteomic analysis. Mass spectrometry data were then subjected to quality control checks, including protein coverage, protein mass, mass tolerance distribution (dmass).

The statistics of all the identified proteins based on their relative molecular weight are shown in Fig. 1A. The molecular weight (MW) of 463 identified proteins (74.56%) ranged from 20 kDa to 120 kDa, and 58 proteins (9.34%) exceeded 120 kDa. As described in Fig. 1B, identified proteins had good sequence coverage. There were 256 proteins (41.22%) with a sequence coverage higher than 20% and 416 (66.99%) with more than 10% sequence coverage distributions of the identified proteins. Dmass shows the error distribution between the valid and theoretical values of the relative molecular weights of all matched peptides. The relative molecular weights of the peptides have minor errors and reliable results (Fig. 1C).

3.3. Analysis of abundant differential proteins (DAPs)

3.3.1. DAPs and correlations

In this study, DAPs were identified based on two criteria of "Fold Change (FC) > 1.2 or FC < 0.83 and *p*-value <0.05". These 240 proteins were identified as DAPs in 10 day/0 day, 20 day/0 day and 30 day/0 day groups. As shown in the Upset graph (Fig. 2A), 83 DAPs were shared proteins among the three groups. There were 22, 15, 38 shared DAPs in the 10 day/0 day group and 20 day/0 day group, 10 day/0 day group and 30 day/0 day group, 20 day/0 day group and 30 day/0 day group, respectively. In addition, there were 28, 31, 23 exclusive DAPs in the 10 day/0 day group, 20 day/0 day group, 30 day/0 day group, respectively. Indicator proteins should be present throughout the storage cycle; therefore, 83 shared DAPs in all groups were analyzed.

As illuminated in Fig. 2B, the circle of the chord diagram has the sample name on one side and the protein ID on the other side, and the connecting line indicates the corresponding protein of the sample. The thicker the line segment, the higher the protein abundance. As diagram shows the DAPs with the top 20 proteins abundance. The top ten with the highest protein abundance are K4Q2S1, K4Q111, A0A3R7PTG0, B4YAH6, C7A639, A0A3R7PBR0, A0A3R7P0W1, A0A423SVE3, A0A4Y5R070, A0A423T857.

3.3.2. Biological process for exclusive DAPs

The exclusive DAPs were analyzed for functional enrichment to understand the role of these proteins in each group. As described in Fig. 3A–C, this analysis revealed the Gene Ontology (GO) secondary entries and their protein numbers in the top five GO annotations and the pathways with more than five Kyoto Encyclopedia of Genes and Genomes (KEGG) enriched pathway proteins. The two functions of cellular process and metabolic process in BP annotation were present in all three comparison groups, in addition to the catalytic activity, binding, biological regulation of these proteins, and the metabolic pathways and ribosomes in the KEGG pathway may be related to the muscle quality during freezing storage (He et al., 2018). Collectively, exclusive DAPs had the same function during storage, affect the maintenance of muscle protein stability.

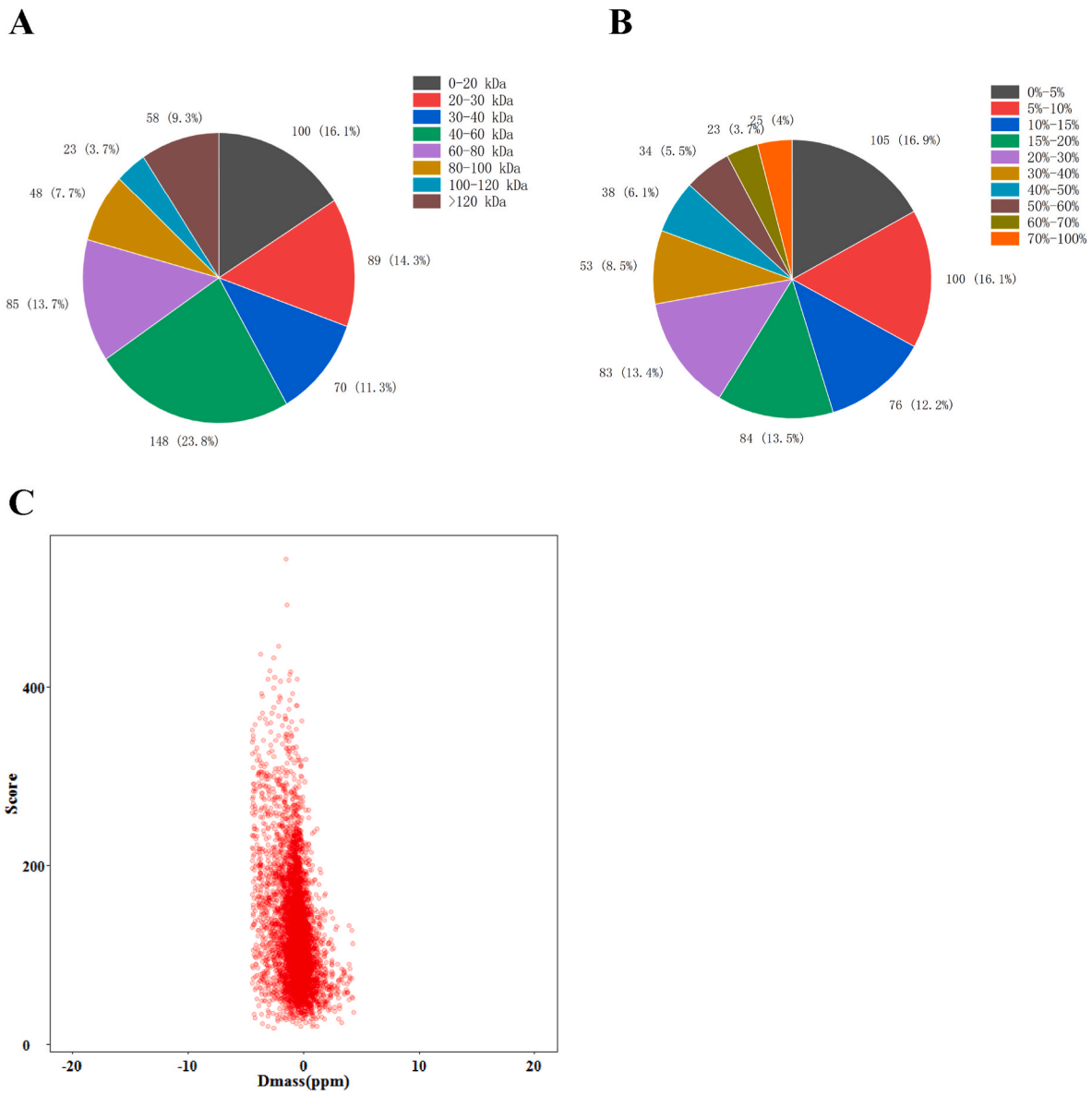

Fig. 1. (A) Protein coverage, (B) protein mass, and (C) protein dmass of proteome of *L. vannamei* during partial freezing.

3.3.3. *Protein description of shared DAPs*

The DAPs that could be identified in all groups may represent the fundamental responses in shrimp muscles during the storage time. Except for 7 uncharacterized proteins, 4 putative proteins, and 2 variable irregular proteins because the functions have not been determined, 70 shared DAPs were analyzed. As illuminated in Table 2, 52 were down-regulated proteins and 18 were up-regulated proteins. GO annotation and KEGG enrichment analysis were performed on the shared proteins, and Fig. 3D shows the GO secondary entries and KEGG enrichment pathway proteins in the top five annotations in shared DAPs. GO annotations are mainly distributed in nucleotide binding, metal ion binding, ATP binding, transferase activity, oxidoreductase activity. In KEGG enrichment, salmonella infection and pathogenic escherichia coli infection are associated with quality deterioration during storage.

During storage of shrimp muscle, proteins underwent denaturation, oxidation (Chen et al., 2020), degradation (Qian et al., 2015), and color changes (Lee et al., 2022), as well as changes in the tenderness and water-holding capacity (Okpala 2015) of the shrimp muscle. Among the DAPs shown in Table 1, related proteins are also associated with quality. The related proteins were analyzed to find proteins that could serve as indicators of shrimp muscle quality changes. As described in Fig. 4A and B, the FC change and protein stability of the indicator proteins, respectively.

3.4. *Proteins related to protein denaturation and oxidation*

The degree of protein denaturation and oxidation is one of the main factors causing changes in the quality of processed aquatic products, related to the storage temperature and the length of storage time (Chen et al., 2020). Protein denaturation leads to the exposure of amino acid residues and the oxidation of some amino acids. In turn, protein oxidation modifies amino acid residues, promoting protein denaturation. Moreover, protein oxygen denaturation and oxidation are closely linked. According to the relevant literature, projectin, ribosomal proteins (Zhang et al., 2020b), and histones (Ji et al., 2021) had changes associated with protein denaturation and oxidation.

Projectin is an elastic filament-linker protein found in arthropod rhabdomyosis, related to twitchin and titin. A0A423T5K0 is defined as projectin, simultaneously was the shared differential abundant protein at 10 day/0 day, 20 day/0 day, and 30 day/0 day, showed a down-

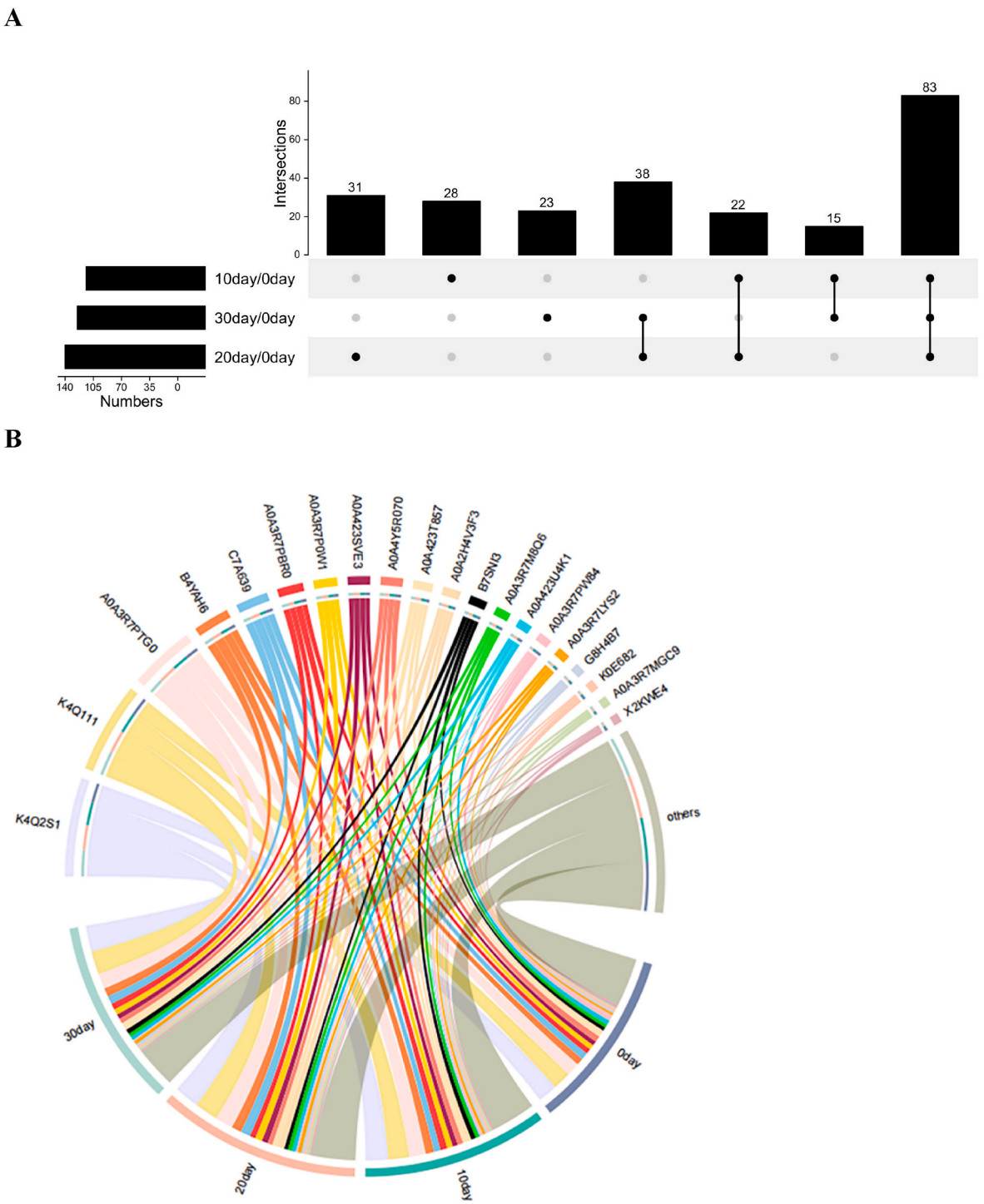

Fig. 2. (A) UpSet diagram and (B) chord diagram of DAPs of *L. vannamei* during partial freezing.

regulation trend (Fig. 4A). The instability index was 48.24 illuminated that it is not stable in vitro and prone to degradation (standard <40 for stable proteins) (Fig. 4B). Ji et al. (2021) found in a study of New Prawns with Knife (*Metapenaeus ensis)* that projectin was confirmed to be down-regulated in both F18-CON and F60-CON comparisons, revealed projectin levels were negatively correlated with protein denaturation and oxidation. Therefore, increased denaturation and oxidation of proteins under low-temperature storage conditions reduce projectin extractability. Shi et al. (2018) also reported a down-regulation of projectin in mud shrimp (*Solenocera melantho*). Muscle connectivity properties and contractility were decreased, causing decreased elasticity (Zhang et al., 2020b).

In muscle tissue, ribosomes consist of a small 40S subunit and a large 60S subunit since they are complex organelles. The three comparison groups described the shared differential abundant proteins A0A3R7MSS7 and A0A076NBT3 by the three comparison groups as 40S ribosomal protein S7 and 60S ribosomal protein L40. As showed in Fig. 4A, these two ribosomal proteins illuminated a down-regulation trend in abundance. A0A3R7MSS7 and A0A076NBT3 instability index were 34.43 and 37.07 revealing it is a stable protein (Fig. 4B). Ribosomal proteins are involved in protein synthesis and maintain tRNA stability during transcription. Zhang et al. (2020b) showed that the 40S and 60S

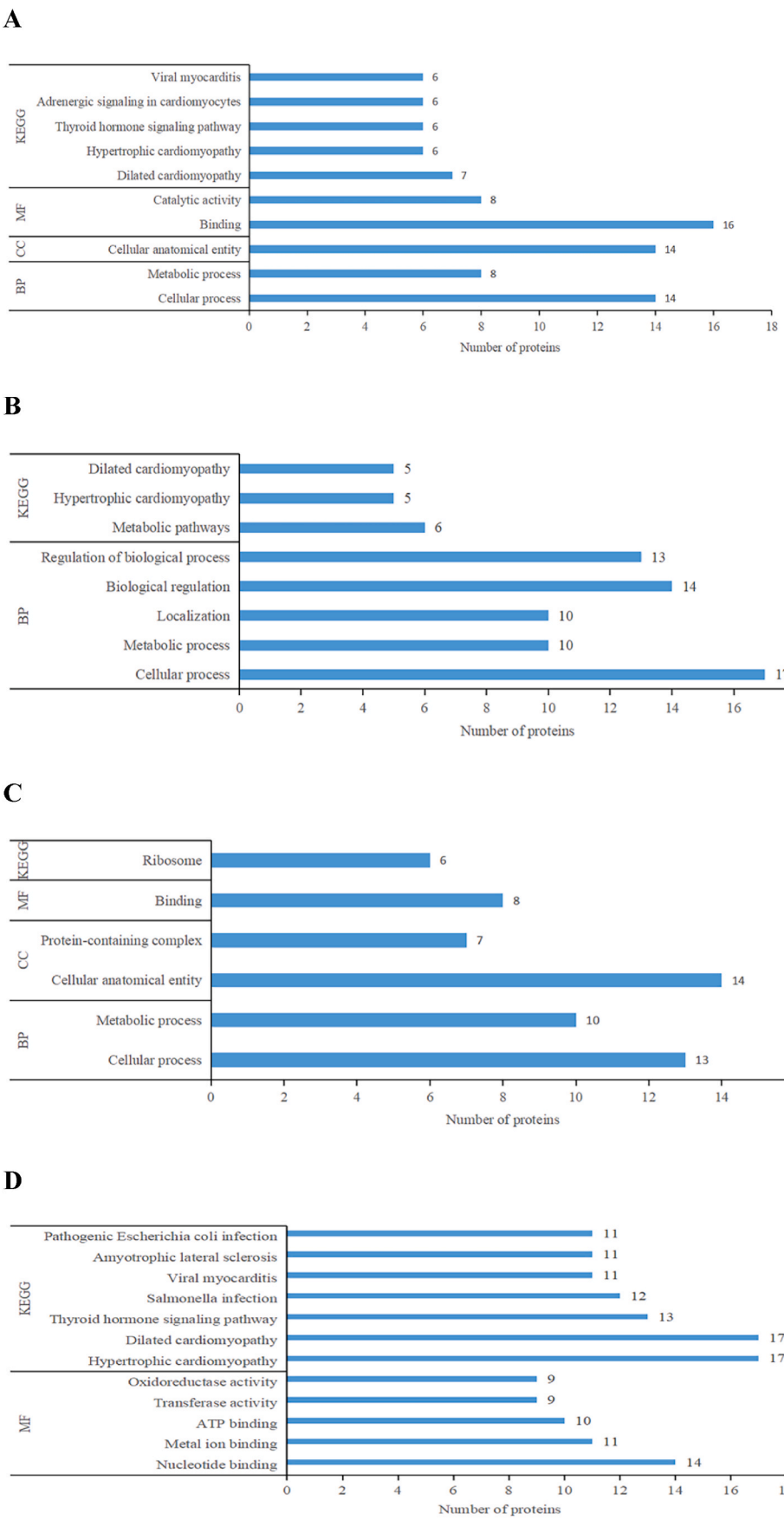

Fig. 3. Top five Gene Ontology terms and KEGG pathways enriched with exceeding five number of proteins (A) 10 day/0 day, (B) 20 day/0 day, and (C) 30 day/0 day of exclusive DAPs of *L. vannamei* during partial freezing when 0 day was controlled sample and 10 day, 20 day, 30 day were experimental group. Ontology terms:MF - Molecular Function; CC - Cellular Component; BP- Biological Process. (D) GO terms and KEGG enrichment pathway proteins in the top five annotations of shared DAPs of *L. vannamei* during partial freezing.

Table 2
The all significantly decreased and increased proteins in 10 day/0 day, 20 day/0 day and 30 day/0 day of *L. vannamei* during partial freezing.

Accession	Mass [kDa]	FC (10day/0day)	FC (20day/0day)	FC (30day/0day)	p (10day/0day)	p (20day/0day)	p (30day/0day)	Protein Des.
A0A3R7M961	17.334	0.085	0.091	0.062	0.002	0.002	0.005	Myosin light chain
A0A3R7QRP4	20.432	0.302	0.188	0.162	0.002	0.002	0.004	Muscle LIM protein Mlp84B
A0A423U2N3	71.592	0.334	0.675	0.456	0.001	0.019	0.011	Calphotin (Fragment)
A0A3R7MDX3	75.196	0.334	0.293	0.358	0	0.001	0.002	LAM_G_DOMAIN domain-containing protein
A0A423TFS5	103.8	0.337	0.147	0.171	0.016	0.007	0.006	Trehalose-6-phosphate synthase
A0A423U528	19.097	0.352	0.185	0.255	0.006	0	0	Crustacyanin-A
A0A3S5HJG4	50.454	0.374	0.446	0.444	0.001	0.003	0.012	Tubulin beta chain
A0A423TIS3	21.026	0.389	0.322	0.322	0.003	0.002	0.004	Heat shock protein
A0A423TEC0	32.776	0.393	0.44	0.446	0.027	0.015	0.022	ATP-dependent (S)-NAD(P)H-hydrate dehydratase
Q1ALB5	31.516	0.439	0.439	0.583	0.016	0.003	0.006	Farnesoic acid O-methyltransferase isoform
A0A423U8M4	49.066	0.441	0.428	0.404	0.001	0.001	0	Tubulin alpha chain
A0A075DVX7	35.67	0.449	0.171	0.309	0.024	0.006	0.016	Activated protein kinase C receptor (Fragment)
A0A3R7PEZ1	41.73	0.467	0.528	0.27	0.023	0.036	0.032	Actin 1
A0A423SMS3	52.845	0.485	0.521	0.534	0.019	0.002	0.014	Tubulin beta chain
A0A3R7MSS7	27.129	0.487	0.232	0.223	0.01	0.008	0.009	40S ribosomal protein S7
A0A3R7QFV3	41.766	0.487	0.361	0.317	0.011	0.001	0.004	Actin T2
A0A423TH89	96.906	0.496	0.474	0.398	0.005	0.042	0.003	Muscle LIM protein Mlp84B
A0A423U095	60.829	0.502	0.482	0.503	0.002	0.002	0.028	Muscle M-line assembly protein unc-89
A0A3R7NX50	41.715	0.511	0.478	0.587	0.005	0.002	0.037	Actin 1
A0A423SG07	19.006	0.535	0.318	0.224	0.019	0.009	0.004	ATP synthase subunit d, mitochondrial
A0A3R7PW84	49.928	0.545	0.354	0.276	0.002	0	0	Glyceraldehyde-3-phosphate dehydrogenase
A0A076NBT3	14.701	0.558	0.349	0.429	0.011	0.035	0.005	60S ribosomal protein
A0A2H4V3E4	41.894	0.56	0.539	0.41	0.031	0	0.007	Actin 1
A0A3R7MS58	50.742	0.563	0.525	0.544	0.007	0.005	0.007	Tubulin beta chain
S4VEU6	31.561	0.58	0.435	0.623	0.034	0.01	0.009	Superoxide dismutase
A0A423SLW8	24.833	0.594	0.44	0.426	0.005	0.002	0.002	Malate dehydrogenase
A0A3R7PMB6	58.966	0.597	0.37	0.451	0.013	0.005	0.005	Adenylyl cyclase-associated protein
A0A3R7LWS7	35.109	0.61	0.462	0.435	0.03	0.027	0.033	Poly(U)-specific endoribonuclease
A0A3R7M776	12.483	0.62	0.629	0.53	0.01	0.011	0.03	Histone H2A
A0A411FUZ0	11.381	0.623	0.454	0.429	0.006	0	0.047	Histone H4
A0A2H4V3C6	41.835	0.625	0.524	0.539	0.017	0.011	0.014	Cytoplasmic-type actin 3
A0A3R7SZS6	49.746	0.634	0.568	0.669	0.021	0.033	0.028	Isocitrate dehydrogenase [NADP]
A0A423TE44	170.36	0.637	0.592	0.586	0.011	0.009	0.004	Fibril-forming collagen alpha chain-like
K7X7H6	24.219	0.64	0.405	0.406	0.002	0.013	0.001	Troponin I
A0A423SYM7	52.056	0.641	0.411	0.461	0.009	0.005	0.002	Citrate synthase
A0A3R7M5U5	38.128	0.645	0.482	0.494	0.033	0.007	0.032	Sodium potassium-transporting ATPase subunit beta
A0A423SNX9	477.65	0.653	0.615	0.57	0	0.001	0	I-connectin
A0A3R7NSY1	314.71	0.653	0.64	0.606	0.001	0.001	0.003	I-connectin
A0A3R7MD67	134.8	0.685	0.494	0.568	0.022	0.009	0.009	4-alpha-glucanotransferase (Fragment)
I1VSB4	36.022	0.685	0.503	0.711	0.002	0.001	0.011	L-lactate dehydrogenase
A0A423T5K0	88.01	0.696	0.682	0.736	0.003	0.005	0.006	Projectin
A0A423T180	101.23	0.707	0.645	0.718	0.006	0.001	0.001	Phosphofructokinase
A0A3R7SMK3	27.37	0.719	0.492	0.615	0.025	0.002	0.005	Glutathione S-transferase
A0A423T9T8	78.441	0.722	0.533	0.478	0.002	0	0.002	Glycogen debranching enzyme
X2KWE4	74.989	0.736	0.733	0.693	0.029	0.011	0.012	Hemocyanin
A0A423U3M3	45.511	0.737	0.54	0.498	0.01	0.004	0.001	Aspartate aminotransferase
A0A3R7PUW0	19.864	0.749	0.564	0.602	0.01	0.003	0.008	SHSP domain-containing protein OS
A0A3R7Q0U0	62.01	0.758	0.336	0.35	0.036	0.02	0.002	Methenyltetrahydrofolate synthase domain-containing protein
A0A0D3QZ08	36.26	0.771	0.689	0.78	0.015	0.002	0.002	Fructose-bisphosphatase
B6RHH5	63.781	0.8	0.832	0.788	0.003	0.007	0.017	Pyruvate kinase
A0A3R7Q123	77.358	0.83	0.693	0.714	0.035	0.034	0.012	Hemocyanin
A0A423TF99	287.22	0.833	0.791	0.822	0.02	0.014	0.024	I-connectin
A0A423U4K8	87.641	5.196	12.601	5.313	0.001	0	0.003	Myosin heavy chain type a
A0A3R7PYS0	587.72	3.453	3.817	3.821	0.002	0.007	0	Nesprin-1-like
A0A3R7NZC3	33.075	2.657	3.562	3.968	0.043	0.003	0.003	Sarcoplasmic calcium-binding protein variant a
A0A3R7NX66	41.815	2.346	4.297	1.887	0.002	0.011	0.006	Actin 2
A0A423U7N4	10.89	1.904	2.076	1.91	0.006	0.011	0.019	Troponin C
A0A3R7M4R5	61.842	1.884	1.515	1.72	0.025	0.034	0.008	Slow muscle myosin S1 heavy chain
A0A3R7PJ50	77.179	1.847	1.853	1.521	0.001	0.001	0.042	Myosin heavy chain type 2
A0A088MK65	76.79	1.804	1.603	1.367	0.007	0.022	0.032	Hemocyanin
A0A3R7MGC9	80.922	1.803	2.538	2.054	0.001	0	0.03	Myosin heavy chain type 1
A0A3R7MHL2	49.245	1.795	2.027	1.926	0.012	0.003	0.007	Basement membrane-specific heparan sulfate proteoglycan core protein
A0A423SGU8	152.11	1.536	2.183	1.739	0.001	0.001	0.002	Hemocyanin subunit L2
A0A3R7SS49	23.99	1.507	1.473	1.448	0.006	0.004	0.004	Alpha-actinin, sarcomeric
A0A423U9Z8	55.53	1.387	1.367	1.889	0.025	0.004	0.01	Ryanodine receptor
A0A3R7MZV2	38.465	1.359	1.876	1.742	0.007	0.025	0.02	Phosphate carrier protein, mitochondrial
A0A423SPG0	41.831	1.324	6.467	3.26	0.021	0	0.003	Actin 2
A0A3R7LYS2	84.528	1.317	1.674	1.643	0.01	0.005	0.005	Myosin heavy chain type 2
B4YAH6	32.849	1.222	1.413	1.243	0.009	0.003	0.009	Lit v 1 tropomyosin

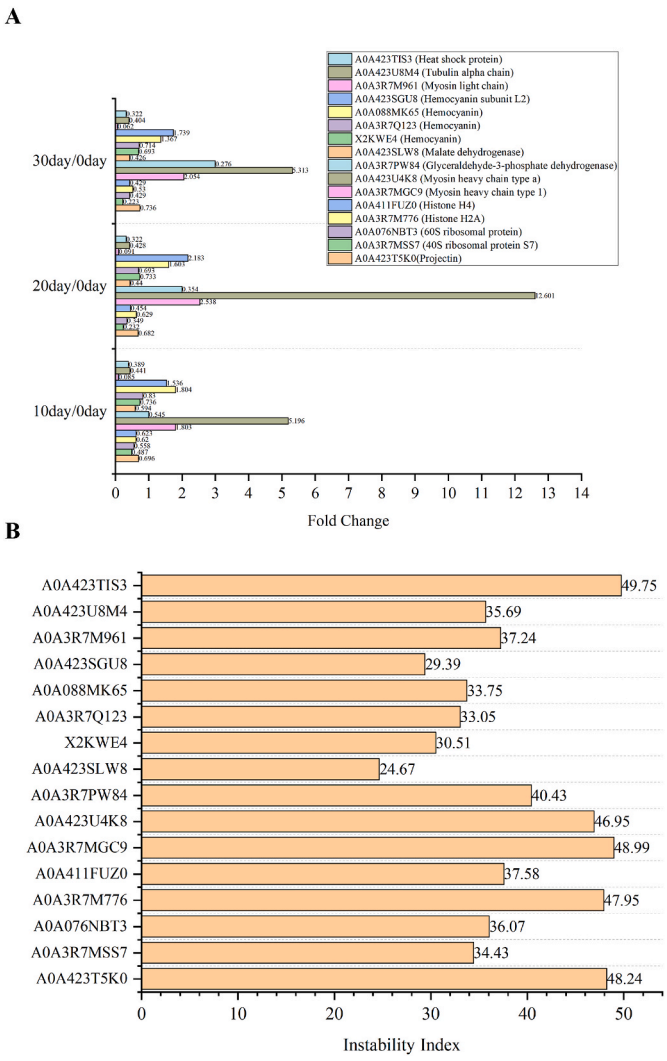

Fig. 4. The fold change, protein instability index of indicators proteins and amino acid composition, hydrophilicity diagram of tenderness and water holding capacity indicators proteins. (A) Fold change of indicators proteins; (B) protein instability index of indicators proteins; (C) amino acid composition of tenderness and water holding capacity indicators proteins, (D) hydrophilicity diagram of myosin light chain, (E) hydrophilicity diagram of tubulin alpha chain and (F) hydrophilicity diagram of heat shock protein of *L. vannamei*.

ribosomal proteins of shrimp soaked in distilled water were down-regulated during storage at −18 °C for 30 days which may be related to the decrease in extraction rate due to protein denaturation.

Histones are major protein components of chromatin and can regulate gene expression (Storey, 2015). In a proteomic study of razor clams, it was found that histone H2A (A0A0B7AUT8) and histone H3 (K0J732) were down-regulated in abundance after 11 days of storage at −1.5 °C, suppressing gene expression in the process (Wang et al., 2018). The shared differential abundant proteins A0A3R7M776 and A0A411FUZ0 to the three compared groups, respectively, express histone H2A and H4; meanwhile, down-regulation of both proteins occurred (Fig. 4A). Possible reasons for the down-regulation of proteins are probably due to the formation of ice crystals during partial freezing. Furthermore, the destructive effect of recrystallization on histone leads to the labile degradation of this protein.

3.5. Proteins related to protein degradation

Protein degradation results from a series of physicochemical reactions combined with microbial growth over time. The degradation of protein directly leads to the softening of aquatic muscle and the gradual loss of various functional properties of muscle tissue, including textural properties (Subbaiah et al., 2015).

Myosin heavy chain is the main structural and functional protein in muscle; the main component proteins are myosin heavy chain type a (MHC a), myosin heavy chain type b (MHC b), and myosin heavy chain type 1 (MHC 1). All three proteins are essential and vital components of myofibrillar proteins; simultaneously, they are responsible for the structural integrity of skeletal muscle involved in muscle contraction and relaxation (Tian et al., 2016). The molecular weights of MHC 1 (A0A3R7MGC9) and MHC a (A0A423U4K8), respectively 81 kDa, 88 kDa; the instability index, respectively 48.99 and 46.95, illuminated that they are not stable in vitro and prone to degradation (Fig. 4B). Meanwhile, the abundance of differential proteins is up-regulated, especially the abundance of A0A423U4K8 was adjusted downward more (Fig. 4A). The higher up-regulation of abundance and the possible reason for the increased abundance is due to the degradation of intact myosin and protein hydrolysis.

Glyceraldehyde-3-phosphate dehydrogenase (GAPDH) is a metabolic enzyme and multifunctional protein. During glycolysis, 3-phosphoglyceraldehyde dehydrogenase oxidizes and phosphorylates with NAD+ and inorganic phosphate (Pi) to produce 3-phosphoglyceraldehyde.

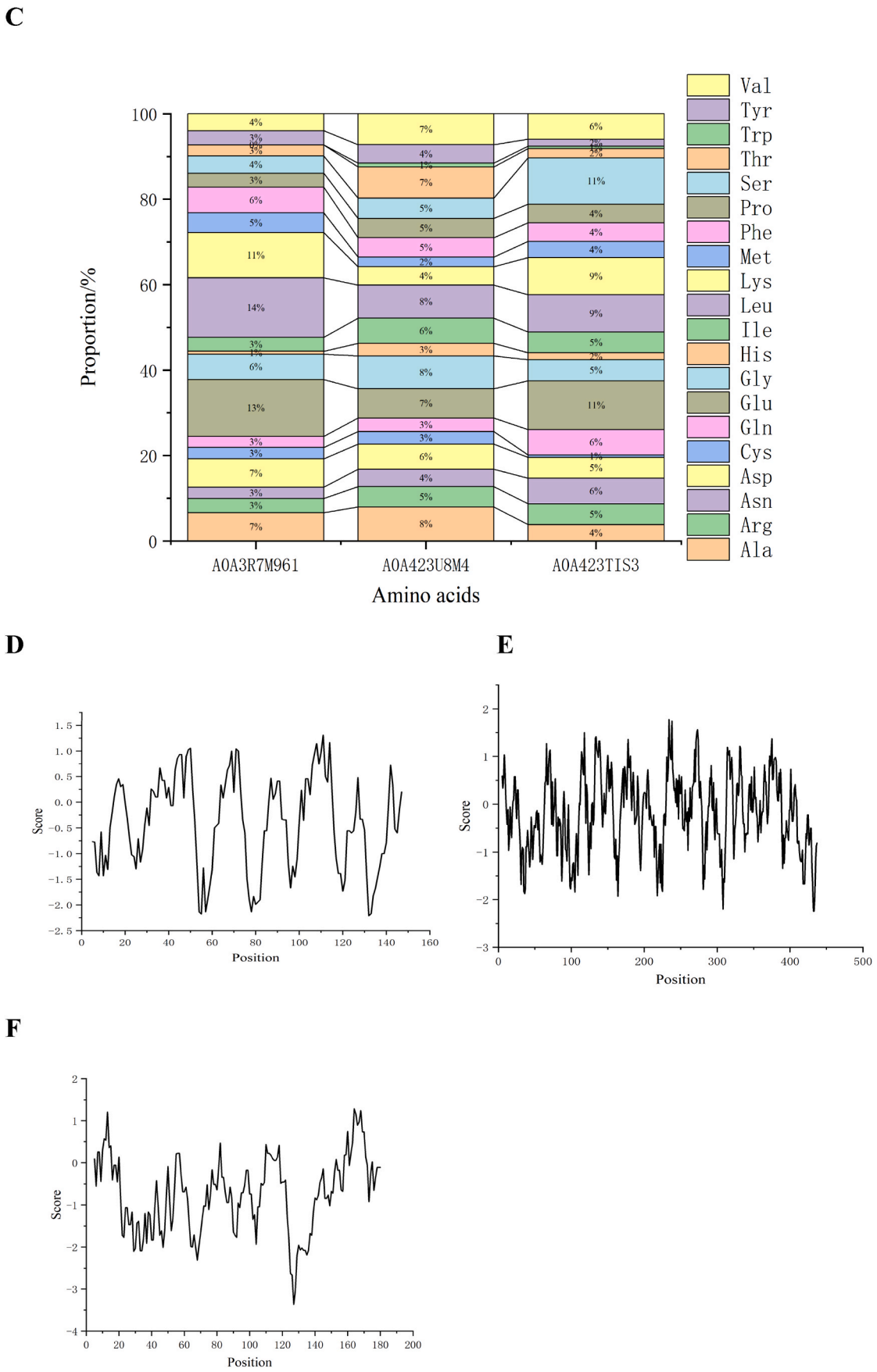

Fig. 4. (*continued*).

Glyceraldehyde 3-phosphate generates 1,3-diphosphoglyceric acid and reduced NADH (Cho et al., 2012). A0A3R7PW84 is defined as GAPDH having a molecular weight of approximately 50 kDa and an instability coefficient of 40.43, revealing it is an unstable protein. This protein of FC (10 day/0 day: 0.545; 20 day/0 day: 0.354; 30 day/0 day: 0.276) showed a down-regulation trend, and the down-regulation might be related to the disappearance of glycogen and its oxidative degradation (Fig. 4A).

3.6. Proteins related to color

The color and appearance of muscle in food products is critical in terms of consumer acceptability at the point of sale. During storage, enzyme oxidation and pigment-binding proteins affect the color of muscle.

Malate dehydrogenase (MDH) catalyzes the reversible conversion between malate and oxaloacetate. It plays a key role in the TCA cycle and glycolysis. At the same time, it is an important enzyme related to color stability (Gao et al., 2016). A0A23SLW8 is defined as MDH with a molecular weight of 25 kDa and FC (10 day/0 day: 0.594; 20 day/0 day: 0.440; 30 day/0 day: 0.426) showed a downward trend (Fig. 4A). The oxidation of MDH accelerated the color change. A negative correlation between MDH and a* values during post-slaughter storage of beef muscle has been reported; thus, its change affected the muscle color (Wu et al., 2016).

Crustacyanin is a protein whose color change is caused by the pigment release due to the denaturation of pigment-binding proteins. Its color change is associated with pigment-binding proteins composed of hemocyanin. Hemocyanin is a respiratory protein with oxygen transport and internal defense functions; simultaneously, it can bind to pigments and is involved in the color change of the shell of *L. vannamei* (Pan et al., 2019). As illuminated in Fig. 4A, the proteins of X2KWE4 and A0A3R7Q123 were down-regulated proteins; A0A088MK65 was up-regulated proteins. According to Tables 2 and X2KWE4, A0A3R7Q123 and A0A088MK65 were described as hemocyanins. In addition, there was a hemocyanin subunit L2 (A0A423SGU8) with a molecular weight of 152 kDa. The abundance of hemocyanin (A0A088MK65) and hemocyanin subunit L2 (A0A423SGU8) were up-regulated. It has been shown that more hemocyanin accumulates from the shrimp exoskeleton in the epidermis. They play an essential role in the hardening, and pigmentation of the cuticle shrimp shell is more prone to blackening (Adachi et al., 2005). The abundance of hemocyanin (X2KWE4; A0A3R7Q123) was down-regulated. The downward adjustment of protein is that a portion of hemocyanin is derived from polyphenol oxidase (PPO) (Adachi et al., 2005). At the same time, PPO derived from shrimp muscle is released, and the melting of ice crystals is more favorable to promoting the contact between hemocyanin and blackening synergists (Nirmal and Benjakul, 2010).

3.7. Proteins related to tenderness and water holding capacity (WHC)

Muscle tenderness is one of the characteristics that consumers are highly concerned it. Water holding capacity refers to the ability of food to maintain its moisture during storage, transportation, and cooking. The loss of water in the muscle will lead to the loss of some water-soluble proteins and nutrients and affect the tenderness and flavor of the muscle (Pearce et al., 2011).

Myosin is an abundant protein in skeletal muscle protofibrils. Therefore, it must be considered when defining the mechanism of muscle tenderization (Pearce et al., 2011). In the study of Zhang et al. (2021), the proteins most likely to act as indicators of muscle tenderness and water holding capacity include the myosin light chain and tubulin alpha chain. Myosin light chain (A0A3R7M961), tubulin alpha chain (A0A423U8M4) were down-regulated in abundance, whose FC were 0.085, 0.091, 0.062 and 0.441, 0.428, 0.404 in 10 day/0 day, 20 day/0 day, 30 day/0 day, respectively (Fig. 4A). The formation of ice crystals produced by partial freezing led to the changes in the distribution, orientation, particle size, and shape of muscle tissue during storage. These changes induce subsequent aggregation, cross-linking, rearrangement, and irreversible denaturation of muscle proteins, leading to rupture and structural disruption of myogenic fibers (Zhang et al., 2020a; Fernández et al., 2008) and a decrease in the tenderness and water holding capacity of shrimp muscle.

Heat shock proteins (HSP) are inductively expressed stress proteins with anti-apoptotic effects and chaperone functions. Simultaneously, HSP interacts with membrane lipids, maintains membrane integrity and function, and is closely associated with WHC in muscles (Zhang et al., 2017). The FC of heat shock protein (A0A423TIS3) (10 day/0 day: 0.389; 20 day/0 day: 0.322; 30 day/0 day: 0.322) was down-regulated, demonstrating a loss of cell membrane integrity and a decrease in water-holding capacity (Fig. 4A). Similarly, related literature reported that the decline in goat muscle was associated with the down-regulation of HSP, which decreased HSP content, leading to structural damage of muscle fibers, therefore a decrease in the water-holding capacity of the muscle (Wang et al., 2016).

A0A3R7M9619 has a molecular weight of 17 kDa, and it consists of 151 amino acids, with Leu, Glu, and Lys being a few of the higher proportions (Fig. 4C). A0A423U8M4 has a molecular weight of 49 kDa and constitutes 441 amino acids, with Ala, Gly and Leu being some of the more abundant amino acids. A0A423TIS3 has a molecular weight of 21 kDa and comprises of 184 amino acids, with Glu, Ser and Leu being the top three amino acids. The hydrophobicity results of the three proteins were analyzed by their gene sequences applied Protscale. A0A3R7M961 (Fig. 4D), A0A423U8M4 (Fig. 4E) and A0A423TIS3 (Fig. 4F) had the strongest hydrophobicity of 1.311, 1.778, and 1.289 and the strongest hydrophilicity of −2.211, −2.244, and −3.367. The amino acids of the three proteins were primarily distributed in the hydrophilic region and were predicted to be hydrophilic proteins. The hydrophobic interactions between hydrophobic amino acids are the leading force in maintaining the structural stability of proteins, and the hydrophilic distribution of proteins can reflect the folding of proteins. During partial freezing conditions, the amino acid residues of the hydrophilic side chains exposed on the protein surface are easily affected and weaken the protein's structurally stable. The protein is susceptible to degradation and other activities (Chen et al., 2020).

4. Conclusion

In this study, a label-free proteomics analysis was applied for the protein changes of the shrimp muscle during 10, 20, and 30 days of partial freezing storage. A total of 612 proteins were identified, including 240 DAPs. The carbonyl content reflected oxidized and denatured, TCA soluble peptide considered protein degraded, MFI considered as tenderness, water was lost, the color was changed indicate that the quality deterioration during partial freezing storage. Meantime, projectin, ribosomal protein and histone were identified as the indicator proteins of protein oxidization and denaturation. Myosin heavy chain and glyceraldehyde-3-phosphate dehydrogenase were the potential proteins of protein degradation. In addition, malate dehydrogenase and hemocyanin were potential indicators of color. Meantime, while myosin light chain, tubulin alpha chain, and heat shock protein were potential indicators of tenderness and water holding capacity. Further validation of the information of these proteins in the future and study of whether they can be used as quality indicator proteins during partial freezing storage is beneficial for shrimp muscle quality and food safety.

CRediT authorship contribution statement

Kangting Sun: Investigation, Writing – original draft, Data curation. **Chuang Pan:** Methodology, Investigation, Data curation, Writing – review & editing, Supervision. **Shengjun Chen:** Project administration, Funding acquisition, Writing – review & editing. **Shucheng Liu:**

Conceptualization, Methodology. **Shuxian Hao:** Formal analysis, Software. **Hui Huang:** Formal analysis, Validation. **Di Wang:** Formal analysis, Validation. **Huan Xiang:** Formal analysis, Validation.

Declaration of competing interest

The authors declare that they have no known competing financial interests or personal relationships that could have appeared to influence the work reported in this paper.

Data availability

Data will be made available on request.

Acknowledgments

This work was partially supported by the Hainan Provincial Joint Project of Sanya Yazhou Bay Science and Technology City (320LH037); National Natural Science Foundation of China (32072147); Guangdong Provincial Special Fund For Modern Agriculture Industry Technology Innovation Teams (2022KJ151); Central Public-interest Scientific Institution Basal Research Fund,CAFS (2020TD69); Guangdong Basic and Applied Basic Research Foundation (2020A1515110360); Research and Development Projects in Key Areas of Guangdong Province, (2021B0202060002).

References

Adachi, K., Endo, H., Watanabe, T., Nishioka, T., Hirata, T., 2005. Hemocyanin in the exoskeleton of crustaceans: enzymatic properties and immunolocalization. Pigm. Cell Res. 18 (2), 136–143. https://doi.org/10.1111/j.1600-0749.2005.00217.x.

Anonymous, 2022. China Fishery Statistics Yearbook of 2022. Chinese Agriculture Press, Beijing, China.

Benjakul, S., Visessanguan, W., Tueksuban, J., 2003. Changes in physico-chemical properties and gel-forming ability of lizardfish (*Saurida tumbil*) during post-mortem storage in ice. Food Chem. 80 (4), 535–544. http://doi:10.1016/s0308-8146(02)00339-4.

Chen, S.J., Tao, F.Y., Pan, C., Hu, X., Ma, H.X., Li, C.S., Zhao, Y.Q., Wang, Y.Q., 2020. Modeling quality changes in Pacific white shrimp (*Litopenaeus vannamei*) during storage: comparison of the Arrhenius model and Random Forest model. J. Food Process. Preserv. 45 (1), e14999. https://doi:10.1111/JFPP.14999.

Cho, H.S., Seo, S.W.W., Kim, Y.M., Jung, G.Y., Park, J.M., 2012. Engineering glyceraldehyde-3-phosphate dehydrogenase for switching control of glycolysis in *Escherichia coli*. Biotechnol. Bioeng. 109 (10), 2612–2619. https://doi:10.1002/bit.24532.

Du, X., Li, H., Nuerjiang, M., Shi, S., Kong, B.H., Liu, Q., Xia, X.F., 2021. Application of ultrasound treatment in chicken gizzards tenderization: effects on muscle fiber and connective tissue. Ultrason. Sonochem. 79, 105786. https://doi:10.1016/j.ultsonch.2021.105786.

Fernández, P.P., Otero, L., Martino, M.M., Molina-García, A.D., Sanz, P.D., 2008. High-pressure shift freezing: recrystallization during storage. Eur. Food Res. Technol. 227 (5), 1367–1377. https://doi:10.1007/s00217-008-0853-7.

Gallart-Jornet, L., Rustad, T., Barat, J.M., Fito, P., Escriche, I., 2007. Effect of superchilled storage on the freshness and salting behavior of Atlantic salmon (*Salmo salar*) fillets. Food Chem. 103 (4), 1268–1281. https://doi:10.1016/j.foodchem.2006.10.040.

Gao, X.G., Wu, W., Ma, C.W., Li, X.M., Dai, R.T., 2016. Postmortem changes in sarcoplasmic proteins associated with color stability in lamb muscle analyzed by proteomics. Eur. Food Res. Technol. 242 (4), 527–535. https://doi:10.1007/s00217-015-2563-2.

He, Y.F., Huang, H., Li, L.H., Yang, X.Q., 2018. Label-free proteomics of tilapia fillets and their relationship with muscle texture during post-mortem storage. Food Anal. Methods 11 (11), 3023–3033. https://doi:10.1007/s12161-018-1273-3.

Ji, W.N., Bao, Y.L., Wang, K.Y., Yin, L., Zhou, P., 2021. Protein changes in shrimp (*Metapenaeus ensis*) frozen stored at different temperatures and the relation to water-holding capacity. Int. J. Food Sci. Technol. 56 (8), 3924–3937. https://doi:10.1111/IJFS.15009.

Jiang, Q., Gao, P., Liu, J.T., Yu, D.W., Xu, Y.S., Yang, F., Wa, B., Yu, P.P., Xia, W.H., 2021. Endogenous proteases in giant freshwater prawn (*Macrobrachium rosenbergii*): changes and its impacts on texture deterioration during frozen storage. Int. J. Food Sci. Technol. 56 (11), 5824–5832. http://doi:10.1111/ijfs.15197.

Lee, Y.C., Tsai, Y.H., Hwang, C.C., Lin, C.Y., Huang, Y.R., 2022. Evaluating the effect of an emerging microwave-assisted induction heating (MAIH) on the quality and shelf life of prepackaged Pacific white shrimp *Litopenaeus vannamei* stored at 4 °C in Taiwan. Food Control 133, 108509. https://doi:10.1016/J.FOODCONT.2021.108509.

Lu, H., Liu, X., Zhang, Y., Wang, H., Luo, Y., 2015. Effects of chilling and partial freezing on *Rigor Mortis* changes of Bighead carp (*Aristichthys nobilis)* fillets: cathepsin activity, protein degradation and microstructure of myofibrils. J. Food Sci. 80 (12), C2725–C2731. https://doi:10.1111/1750-3841.13134.

Lin, H.M., Qi, X.E., Shui, S., Benjakul, S.S., Aubourg, S.P., Zhang, B., 2021. Label-free proteomic analysis revealed the mechanisms of protein oxidation induced by hydroxyl radicals in whiteleg shrimp (*Litopenaeus vannamei*) muscle. Food Funct. 12 (10), 4337–4348. http://doi:10.1039/d1fo00380a.

Liu, Z.Y., Liu, Q.M., Zhang, D., Wei, S., Sun, Q.X., Xia, Q.Y., Shi, W.Z., Ji, H.W., Liu, S.C., 2021a. Comparison of the proximate composition and nutritional profile of byproducts and edible parts of five species of shrimp. Foods 10 (11), 2603. https://doi:10.3390/FOODS10112603.

Liu, Y., Sun, Q.X., Pan, Y.M., Wei, S., Xia, Q.Y., Liu, S.C., Deng, C.J., Hao, J.M., 2021b. Investigation on the correlation between changes in water and texture properties during the processing of surimi from golden pompano (*Trachinotus ovatus*). J. Food Sci. 86 (2), 376–384. https://doi:10.1111/1750-3841.15581.

Nikoo, M., Benjakul, S., Rahmanifarah, K., 2016. Hydrolysates from marine sources as cryoprotective substances in seafoods and seafood products. Trends Food Sci. Technol. 57, 40–51. http://doi:10.1016/j.tifs.2016.09.001.

Nirmal, N.P., Benjakul, S., 2010. Effect of catechin and ferulic acid on melanosis and quality of Pacific white shrimp subjected to prior freeze–thawing during refrigerated storage. Food Control 21 (9), 1263–1271. https://doi:10.1016/j.foodcont.2010.02.015.

Okpala, C.O.R., 2015. The physicochemical changes of farm-raised Pacific white shrimp (*Litopenaeus vannamei*) as influenced by iced storage. Food Nutr. Sci. 6 (10), 906. https://doi:10.4236/fns.2015.610095.

Pan, C., Chen, S.J., Hao, S.X., Yang, X.Q., 2019. Effect of low-temperature preservation on quality changes in Pacific white shrimp, *Litopenaeus vannamei*: a review. J. Sci. Food Agric. 99 (14), 6121–6128. https://doi:10.1002/jsfa.9905.

Pearce, K.L., Rosenvold, K., Andersen, H.J., Hopkins, D.L., 2011. Water distribution and mobility in muscle during the conversion of muscle to muscle and ageing and the impacts on fresh muscle quality attributes - a review. Meat Sci. 89 (2), 111–124. https://doi:10.1016/j.musclesci.2011.04.007.

Qian, Y.F., Xie, J., Yang, S.P., Huang, S.L., Wu, W.H., Li, L., 2015. Inhibitory effect of a quercetin-based soaking formulation and modified atmospheric packaging (MAP) on muscle degradation of Pacific white shrimp (*Litopenaeus vannamei*). LWT - Food Sci. Technol. (Lebensmittel-Wissenschaft -Technol.) 63 (2), 1339–1346. https://doi:10.1016/j.lwt.2015.03.077.

Rajagopal, K., Oommen, G.T., 2014. Myofibril fragmentation index as an immediate postmortem predictor of buffalo muscle tenderness. J. Food Process. Preserv. 39 (6), 1166–1171. https://doi:10.1111/jfpp.12331.

Shi, J., Zhang, L.T., Lei, Y.T., Shen, H.X., Yu, X.P., Luo, Y.K., 2018. Differential proteomic analysis to identify proteins associated with quality traits of frozen mud shrimp (*Solenocera melantho*) using an iTRAQ-based strategy. Food Chem. 251, 25–32. https://doi.org/10.1016/j.foodchem.2018.01.046.

Shi, L., Yin, T., Xiong, G.Q., Ding, A., Li, X., Wu, W.J., Qiao, Y., Liao, L., Wang, J., Wang, L., 2020. Microstructure and physicochemical properties: effect of pre-chilling and storage time on the quality of Channel catfish during frozen storage. LWT- Food Sci. Technol. 130, 109606. http://doi:10.1016/j.lwt.2020.109606.

Storey, K.B., 2015. Regulation of hypometabolism: insights into epigenetic controls. J. Exp. Biol. 218 (1), 150–159. https://doi:10.1242/jeb.106369.

Subbaiah, K., Majumdar, R.K., Choudhury, J., Priyadarshini, B.M., Dhar, B., Roy, D., Saha, A., Maurya, P., 2015. Protein degradation and instrumental textural changes in fresh Nile Tilapia (*Oreochromis niloticus*) during frozen storage. J. Food Process. Preserv. 39 (6), 2206–2214. https://doi:10.1111/jfpp.12465.

Tian, X.J., Wu, W., Yu, Q.Q., Hou, M., Jia, F., Li, X.M., Dai, R.T., 2016. Quality and proteome changes of beef *M.longissimus dorsi* cooked using a water bath and ohmic heating process. Innovat. Food Sci. Emerg. Technol. 34, 259–266. https://doi:10.1016/j.ifset.2016.02.013.

Varma, S.D., Devamanoharan, P.S., 1995. Oxidative denaturation of lens protein: prevention by pyruvate. Ophthalmic Res. 27 (1), 18–22. https://doi:10.1159/000267562.

Wang, Z.Y., He, F., Rao, W.L., Ni, N., Shen, Q.W., Zhang, D.Q., 2016. Proteomic analysis of goat *Longissimus dorsi* muscles with different drip loss values related to meat quality traits. Food Sci. Biotechnol. 25 (2), 425–431. https://doi:10.1007/s10068-016-0058-y.

Wang, C., Chu, J., Fu, L.I., Wang, Y.B., Zhao, F., Zhou, D.Q., 2018. iTRAQ-based quantitative proteomics reveals the biochemical mechanism of cold stress adaption of razor clam during controlled freezing-point storage. Food Chem. 247, 73–80. https://doi:10.1016/j.foodchem.2017.12.004.

Wang, C., Wang, H., Li, X., Zhang, C.H., 2019. Effects of oxygen concentration in modified atmosphere packaging on water holding capacity of pork steaks. Meat Sci. 148, 189–197. https://doi:10.1016/j.musclesci.2018.10.001.

Wu, W., Yu, Q.Q., Fu, Y., Tian, X.J., Fei, J., Jia, F., Li, X.M., Dai, R.T., 2016. Towards muscle-specific muscle color stability of Chinese Luxi yellow cattle: a proteomic insight into post-mortem storage. J. Proteonomics 147, 108–118. https://doi:10.1016/j.jprot.2015.10.027.

Xiang, Y., Sun, C.F., Zhao, Y.Q., Li, L.H., Yang, X.Q., Wu, Y.Y., 2022. Label-free proteomic analysis reveals freshness-related proteins in sea bass (*Lateolabrax japonicus*) fillets stored on ice. LWT–Food Sci. Technol. 155, 112885. https://doi:10.1016/J.LWT.2021.112885.

Yang, Z.M., Liu, S.C., Sun, Q.X., Zheng, O.Y., Wei, S., Xia, Q.Y., Ji, H.W., Deng, C.J., Hao, J.M., Xu, J., 2022. Insight into muscle quality of golden pompano (*Trachinotus ovatus*) frozen with liquid nitrogen at different temperatures. Food Chem. 374, 131737. https://doi:10.1016/J.FOODCHEM.2021.131737.

Zhang, M.H., Wang, D.Y., Geng, Z.M., Sun, C., Bian, H., Xu, W.M., Zhu, Y.Z., Li, P.P., 2017. Differential expression of heat shock protein 90, 70, 60 in chicken muscles postmortem and its relationship with muscle quality. Asian-Australasian. J. Anim. Sci. 30 (1), 94. https://doi:10.5713/ajas.16.0132.

Zhang, B., Yao, H., Qi, H., Zhang, X.L., 2020a. Trehalose and alginate oligosaccharides increase the stability of muscle proteins in frozen shrimp (*Litopenaeus vannamei*). Food Funct. 11 (2), 1270–1278. https://doi:10.1039/c9fo02016k.

Zhang, B., Mao, J.L., Yao, H., Santiago, P., Aubourg, S., 2020b. Label-free based proteomics analysis of protein changes in frozen whiteleg shrimp (*Litopenaeus vannamei*) pre-soaked with sodium trimetaphosphate. Food Res. Int. 137, 109455 https://doi.org/10.1016/j.foodres.2020.109455.

Zhang, L., Yin, M.Y., Wang, X.C., 2021. Muscle texture, muscle histochemistry and protein composition of *Eriocheir sinensis* with different size traits. Food Chem. 338, 127632. https://doi:10.1016/j.foodchem.2020.127632.